

Wet mammals shake at tuned frequencies to dry

Andrew K. Dickerson, Zachary G. Mills and David L. Hu

J. R. Soc. Interface published online 17 August 2012
doi: 10.1098/rsif.2012.0429

Supplementary data

["Data Supplement"](#)

<http://rsif.royalsocietypublishing.org/content/suppl/2012/08/17/rsif.2012.0429.DC1.html>

References

[This article cites 42 articles, 6 of which can be accessed free](#)

<http://rsif.royalsocietypublishing.org/content/early/2012/08/16/rsif.2012.0429.full.html#ref-list-1>

P<P

Published online 17 August 2012 in advance of the print journal.

Email alerting service

Receive free email alerts when new articles cite this article - sign up in the box at the top right-hand corner of the article or click [here](#)

Advance online articles have been peer reviewed and accepted for publication but have not yet appeared in the paper journal (edited, typeset versions may be posted when available prior to final publication). Advance online articles are citable and establish publication priority; they are indexed by PubMed from initial publication. Citations to Advance online articles must include the digital object identifier (DOIs) and date of initial publication.

To subscribe to *J. R. Soc. Interface* go to: <http://rsif.royalsocietypublishing.org/subscriptions>

Wet mammals shake at tuned frequencies to dry

Andrew K. Dickerson¹, Zachary G. Mills¹ and David L. Hu^{1,2,*}

¹*School of Mechanical Engineering, and* ²*School of Biology, Georgia Institute of Technology, Atlanta, GA 30332-0405, USA*

In cold wet weather, mammals face hypothermia if they cannot dry themselves. By rapidly oscillating their bodies, through a process similar to shivering, furry mammals can dry themselves within seconds. We use high-speed videography and fur particle tracking to characterize the shakes of 33 animals (16 animals species and five dog breeds), ranging over four orders of magnitude in mass from mice to bears. We here report the power law relationship between shaking frequency f and body mass M to be $f \sim M^{-0.22}$, which is close to our prediction of $f \sim M^{-0.19}$ based upon the balance of centrifugal and capillary forces. We also observe a novel role for loose mammalian dermal tissue: by whipping around the body, it increases the speed of drops leaving the animal and the ensuing dryness relative to tight dermal tissue.

Keywords: allometry; animal size; capillarity; surface tension

1. INTRODUCTION

Water repellency has previously been viewed as a static property of surfaces such as plant leaves and insect cuticle [1,2]. An equally important trait is dynamic water repellency, whereby muscular energy is applied to remove water. This paradigm may have use in sensor design. For example, digital cameras already rely upon internal shakers for removing dust from sensors [3]. Such functionality may have improved the capability of the Mars Rover [4,5], which suffered reduced power from the accumulation of dust on its solar panels. In the future, self-cleaning and self-drying may arise as an important capability for cameras and other equipment subject to wet or dusty conditions.

Many animals evolved physical adaptations to minimize infiltration of water into their furs or feathers [6,7]. Semi-aquatic mammals possess a dense underfur that maintains large air pockets to insulate the body during a dive [8]. Fur itself often has specialized geometries, such as the grooved interlocking hairs of otters that mechanically resist infiltration of water [9]. Certain animals, such as sheep, additionally secrete oily substances such as lanolin that act to increase the hydrophobicity of hair and so discourage fluid–fur contact. In order to arrange their hairs regularly and to uniformly coat them with oil, many animals groom [10] by preening, licking and shaking. Such behaviours may also remove particles in addition to water: birds have been observed to remove dust by shaking after dust-bathing [5] and perform aerial shakes to remove water [11].

Shaking water from an animal surface reduces the combined energetic costs of carrying this water and

evaporating it. Small animals may trap substantial volumes of water in their fur for their size [12–14]: emerging from a bath, a human carries 1 pound of water, a rat 5 per cent its mass and an ant three times its mass. Wet fur is a poor insulator because water's conductivity of $0.6 \text{ W m}^{-1} \text{ K}^{-1}$ is 25 times greater than that of air and 12 times greater than that of dry fur [15], causing a wet animal to lose heat very quickly. Evaporation of the entrapped water from an animal's fur may sap a substantial portion of the animal's energy reserves. The specific energy required [16] is $e = 0.6 \lambda$, where the heat of vaporization of water $\lambda = 2257 \text{ kJ kg}^{-1}$. Consequently, a wet 60-pound dog, with one pound of water in its fur, would use 20 per cent of its daily caloric intake simply to air-dry. It is thus a matter of survival that terrestrial animals remain dry in cold weather [17].

In this study, we investigate a mechanism used by mammals to dry quickly, the wet-dog shake shown in figure 1*a*. We begin §2, with a description of the novel methods developed in this study, including a robotic wet-dog-shake simulator. We proceed by measuring the masses and frequencies of shakes spanning a wide range of mammals. Next, we characterize the kinematics of the shaking response using high-speed video and fur-tracking. We proceed by presenting models for both drop ejection and the ensuing dryness of the animal, testing these models using experiments with a spinning tuft of fur. Lastly, we discuss the implications of our work and suggest directions for future research.

2. MATERIAL AND METHODS

2.1. Animal measurements

We and the Zoo Atlanta staff measured by hand the masses and radii of 28 of the 33 animals in our study.

*Author for correspondence (hu@me.gatech.edu).

Electronic supplementary material is available at <http://dx.doi.org/10.1098/rsif.2012.0429> or via <http://rsif.royalsocietypublishing.org>.

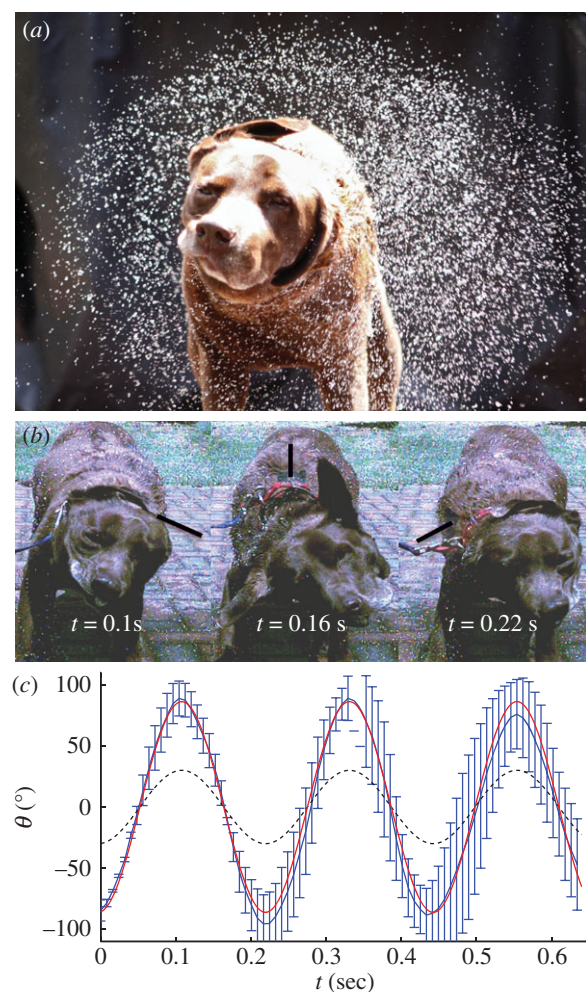


Figure 1. Kinematics of fur during the wet-dog shake. (a) A droplet cloud generated by a Labrador retriever during mid-shake. (b) Time-lapse images of a dog shaking its fur. The thin black line highlights a marker glued between the shoulders of the dog's back. (c) Time course of the angular position of the skin and vertebrae of the dog. Error bars indicate the standard deviation of measurement ($N=3$). Blue solid line, skin; black dashed line, back bone; red solid line, best fit.

The masses and radii of the remaining five animals (squirrel, black bear, brown bear, lion and tiger) were inferred using a combination of methods. Tiger and lion masses were provided by zoo staff from recent veterinary procedures in which the animal was anesthetized and weighed. Chest girth measurements for the tiger and lion were not safely measurable by zoo staff, and were thus inferred from the literature, based on the animals' masses [18,19]. Videos of three species (squirrel, black bear and brown bear) were obtained from YouTube and BBC, where their masses and radii were estimated based on previous measurements of adults in the literature [20–25].

2.2. Wet-dog simulator

We built a 'wet-dog simulator' apparatus to visualize the motion of drops on a shaking mammal. The apparatus is described further in the electronic supplementary

material. 'Dog' fur was provided by three 6.3 cm^2 squares of white-tailed deer tanned fur, which were glued (with non-water-soluble glue) to plastic bases clipped to the rotating axis of our device. Prior to experiments, loose hairs were removed and samples immersed in water for 4 h to ensure complete saturation into skin and fur. Samples were spun for 30 s on the wet-dog simulator at a radius of 2 cm at various frequencies. Between trials, samples were weighed, resaturated with water and drip-dried for 30 s.

2.3. Brush experiments

In order to test Tate's Law, we used 19 brushes with round bases (Loew Cornell Nylon 1812 brushes, Loew Cornell Bristle 1812 brushes and Sterling Studio synthetic brushes SS-100 round set). Originally tapered at a range of slopes, we shaved the brushes to produce a flat tip. We weighed drops dripping from the brushes on an analytical balance. To obtain data in figure 4*d*, three brushes were placed on the 'wet-dog simulator' and the mass of ejected drops at various rotational speeds was determined through image processing with MATLAB. The cylindrical shell method was used to determine the volume of elliptical drops.

3. RESULTS

3.1. Shaking frequencies across mammals

Using high-speed video at 500–1000 fps, we filmed the shakes of 33 wet mammals, spanning 16 species and five breeds of dogs (figure 2). Shakes were prompted by sprinkling small animals with a spray bottle, and large animals with a hose. We found animals generally shook after the flow of water had ceased.

We characterized animal sizes using measurements of body mass M and the chest circumference $2\pi R$ measured posterior to the shoulder, where R is cross-sectional radius of the chest. In general, one specimen per species or breed was available, but several specimens of mice and rats provided the opportunity to determine variability in frequency and mass within a species. The averages and standard deviations of measurements are presented in table 1 with corresponding error bars in figure 3. Among four juvenile mice, four adult mice and four adult rats, the standard deviations for both mass and frequency were only 5–10% of their respective averages, indicating that there is very low variability in these measurements. This also suggests that each animal has a particular frequency at which it shakes.

Figure 3 and table 1 show the relation between frequency of shaking f and animal mass M for the animals in our study. To calculate a best fit, we tried to obtain a fair and uniform sample of the animals studied. The mass and frequency changed little within certain sample groups, such as juvenile mice, adult mice, and adult rats. In these groups, only the average of each group was considered to avoid bias towards particular species in our best fit. Specimens of certain canine breeds such as Labradors and huskies were obtainable in a wider range of masses and so were considered individually rather than as an average for each

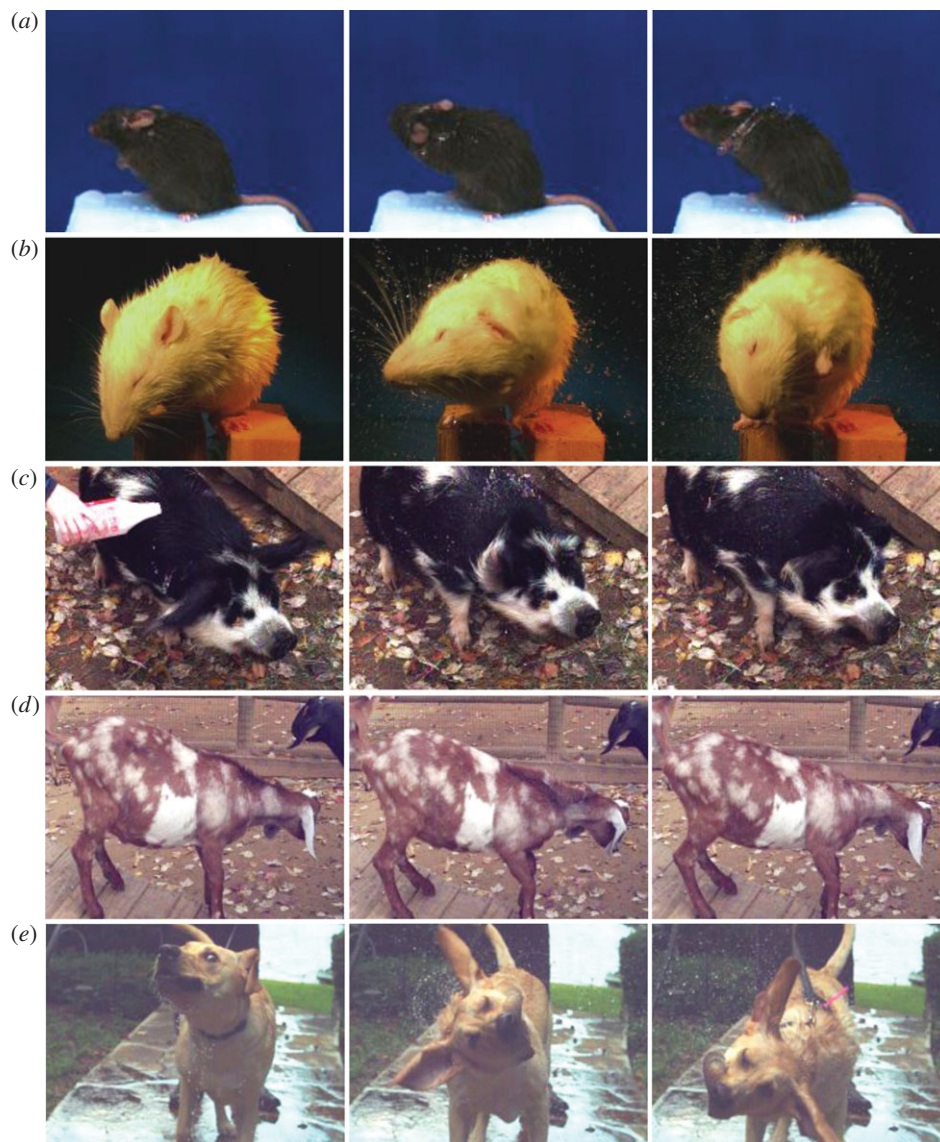


Figure 2. Photo sequences of animals filmed in this study: (a) adult mouse, (b) rat, (c) Kunekune pig, (d) Boer goat and (e) Labrador retriever.

breed. Otherwise, we calculated a best fit using a sample that consisted of one specimen of each canine breed and one specimen of each non-canine species. In all, among the 33 animals measured, we used a sample of 25 data points to determine our best fit.

The best fit using the method of least squares yields

$$f \sim M^{-0.22}, \quad (R^2 = 0.95, N = 25). \quad (3.1)$$

Note that the goodness of fit $R^2 = 0.95$ is high, despite over four orders of magnitude in mass (0.01–260 kg) of the animals considered. Among these animals, we observe a clear dependency of shaking frequency on body size: mice must shake at 30 Hz, dogs at 4.5–8 Hz and bears at 4 Hz.

In figure 3, the vertical distance between the points and the best fit denotes the vigour of the animal's shake with respect to the average. We suspect deviations from the trend are due to modifications in shaking style according to the animal's anatomy, or as in the case of dogs, centuries of domestication. While animals generally shook on four legs, rodents

such as mice and rats stood on hind legs to shake (figure 2*a,b*). Otters and sheep did not shake at frequencies lower than the best fit, as one might expect from the lower adhesion of drops to their waxy fur.

The largest animals such as bears shook at frequencies of 4 Hz, slightly higher than predicted by the best fit (3.5 Hz). Generally, animals in the size range of 4–260 kg exhibited a slightly smaller range in frequency (4–6 Hz) than indicated by the best fit (3.5–9 Hz). This departure from the best fit is likely due to the decreasing importance of shaking with size. The largest animals such as elephants need not shake because of a combination their large thermal mass, thickness of dermal layers and lack of hair. Thus, we expect animals to depart from the observed trends at some critical size, and this departure may in fact begin for the largest animals studied.

3.2. Shaking kinematics

Four Labrador retrievers ($M = 32.5 \pm 6.5$ kg) served as model organisms to characterize the shaking kinematics because they were tame and accessible. A typical shake

Table 1. Size and shaking speeds of animals studied. The radius and mass of the squirrel, black bear and brown bear were estimated from the sizes of average adults in literature [20,21,23,25]. The radii measurements of the lion and tiger were unattainable by the Zoo staff and were estimated similarly sized adults in literature [18,19].

	M mass (kg)	R radius (cm)	F frequency (Hz)	$R\omega^2/g$ non-dimensionalized centrifugal acceleration
mouse weanling <i>Mus musculus</i>	0.01 ± 0.0001	1.2	31.5 ± 2.0	72
adult mouse <i>Mus musculus</i>	0.0272 ± 0.0014	1.3	29.0 ± 1.6	66
rat <i>Rattus norvegicus</i>	0.3077 ± 0.007	2.6	17.869 ± 2.0	53
grey squirrel <i>Sciurus carolinensis</i>	0.50	3.0	15.0	43
guinea pig <i>Cavia porcellus</i>	0.606	3.2	14.1	40
chihuahua <i>Canis lupus familiaris</i>	2.5	5.0	6.8	14
domestic cat <i>Felis catus</i>	3.3	5.9	9.4	33
river otter <i>Amblonyx cinereus</i>	3.5	5.5	10.2	36
poodle <i>Canis lupus familiaris</i>	4.1	5.9	5.6	12
Siberian husky <i>Canis lupus familiaris</i>	10.9	8.8	5.8	19
chow <i>Canis lupus familiaris</i>	15.9	10.0	5.0	16
kangaroo <i>Macropus rufus</i>	19.4	8.1	4.9	12
Siberian husky <i>Canis lupus familiaris</i>	22.3	11.2	5.4	21
Labrador retriever 1 <i>Canis lupus familiaris</i>	26.8	11.9	4.6	16
Labrador retriever 2 <i>Canis lupus familiaris</i>	28.1	12.1	4.5	15
Labrador retriever 3 <i>Canis lupus familiaris</i>	34.0	13.3	4.4	16
Labrador retriever 4 <i>Canis lupus familiaris</i>	41.0	14.1	4.3	17
Boer goat <i>Capra hircus</i>	48.3	13.3	7.7	50
Kunekune pig <i>Sus scrofa</i>	49.4	13.3	8.2	57
Gulf Coast sheep <i>Ovis Aries</i>	55.0	15.0	6.5	40
black bear <i>Ursus americanus</i>	90	15	4.1	16
African lion <i>Panthera leo</i>	114	15	4.8	22
Sumatran tiger <i>Panthera tigris sumatrae</i>	119	16	4.3	19
giant panda <i>Ailuropoda melanoleuca</i>	130	18.1	4.3	21
brown bear <i>Ursus arctos horribilis</i>	260	24	4.0	24

by a Labrador is shown in figure 1*a*, where a fluorescent fiducial marker is taped to the dog's fur in the middle of its back (figure 1*b*). The angular position θ of the marker with respect to the vertical is shown in figure 1*c* and the electronic supplementary material, video S1. We find the shake is closely approximated by simple harmonic motion, in which

$$\theta(t) = A \sin(2\pi ft) \quad (R^2 = 0.98, N = 3), \quad (3.2)$$

where the shake amplitude is $A = 90 \pm 10^\circ$ ($N = 3$) and the frequency (in cycles per second) is $f = 4.5 \pm 0.25$ ($N = 3$). The peak angular velocity of the shake is $\omega = d\theta/dt \sim 2\pi fA$. We observed qualitatively that drops are shed continuously throughout the cycle, with small bursts of increased shedding when the fur changes direction.

We observe in figure 1*b* a surprisingly large amplitude of motion $A \approx 90^\circ$ despite the dog's four paws remaining in contact with the ground. Rotating the

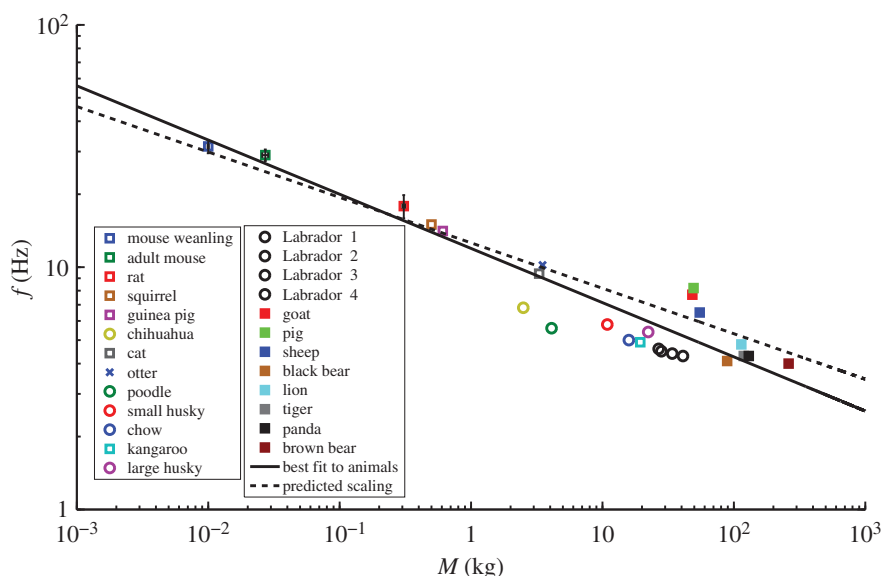


Figure 3. The relation between shaking frequency f and animal radius R . Dogs are denoted by a circle, other mammals by a square and the semi-aquatic otter by an X. Best fit is given in equation (3.1). Error bars indicate the standard deviation of measurement.

dog's skin by hand, while keeping the vertebrae static, indicates that the dermal tissue alone has a maximum deflection of $A_s \approx 60^\circ$. Loose dermal tissue, which roughly contains all substance between fur and muscles, had been previously hypothesized [6] to reduce the energetic cost of locomotion by facilitating limb movement, and we find here it serves another purpose by increasing the amplitude of the shake.

We infer the vertebral motion during the shake has a smaller amplitude $A_v = A - A_s \approx 30^\circ$, as shown by the time course of the dotted line in figure 1c. The vertebral amplitude is three times less than the dermal tissue amplitude during the shake, indicating that loose dermal tissue has an important role in amplifying the shake. We also observed loose dermal tissue in other animals, such as our X-ray videos of rats (see electronic supplementary material, video S2). In our analysis of the forces involved, we will see how this increase in amplitude improves the efficacy of the shake through increasing the centrifugal force on drops within the fur.

3.3. Drops ejection from hair clumps

We now rationalize the observed power law scaling by consideration of the physics of drop release from an animal's furry surface. A wet furry animal will drip water under the influence of gravity. As the animal dries, the falling ligaments of water transform into streams of drops. Because the animal coat is wetting, it is energetically favourable for this departing fluid to follow the animal's hair, from root to tip. Photographs of wet animals such as otters, bears and dogs (see electronic supplementary material and figure 5a) often show wet animal hair forms a fairly uniform series of wet aggregations, resembling wetted paintbrush bristles. These clumps are formed through a complex process that depends on hair spacing, length, curvature, material properties and degree of wetness [26–30]. Tabulated properties [6,31–34] of animal fur properties, including length, diameter, density, and

stiffness, show no dependency on animal size for the range of animal masses we have considered (see electronic supplementary material, figure S1 and S2).

We performed a series of drip tests with variable-sized paintbrushes, ranging in diameter from 1.2 to 11.5 mm meant to simulate the range of hair clump sizes observable in animals. We shaved the tips of the paintbrush bristles flat in order to obtain uniformity in our experiments. The paintbrushes are then suspended in a 'wet-dog simulator' (see electronic supplementary material, figure S5), consisting of a high-strength spinning frame that rotates the brush along with a high-speed camera at a given frequency f . This device allowed us to visualize the flow of fluid as if a dog is shaking at the frequency the device is spun.

3.4. Visualization of drop release

The detachment of drops may be clearly visualized using our system. Figure 4a shows a video sequence of drop release from a paintbrush under gravity. The corresponding drop release from a spinning brush (at 2.61 ms^{-1} with rotation rate of 610 r.p.m.) is shown in figure 4b, and is visually similar to release due to gravity. In both processes, fluid entrained from the brush engorges the drop. This engorgement occurs at a rate that depends on the remaining moisture content of the brush and the applied centrifugal or gravitational forces. During engorgement, the drop remains pinned to the brush. In figure 4a, pinning occurs at the circumference of the hair clump, whereas in figure 4b, at points within the center of clump. Once the drop has grown to a critical size, the pinch-off and release process is quite fast, occurring within 10 ms. In both gravitational- and centrifugal-force-driven dripping, a portion of the drop remains attached to the clump after release.

This phenomenon of drop release has been well-studied in dripping from capillaries [35,36] in the context of intravenous drug delivery and in spinning disk spray

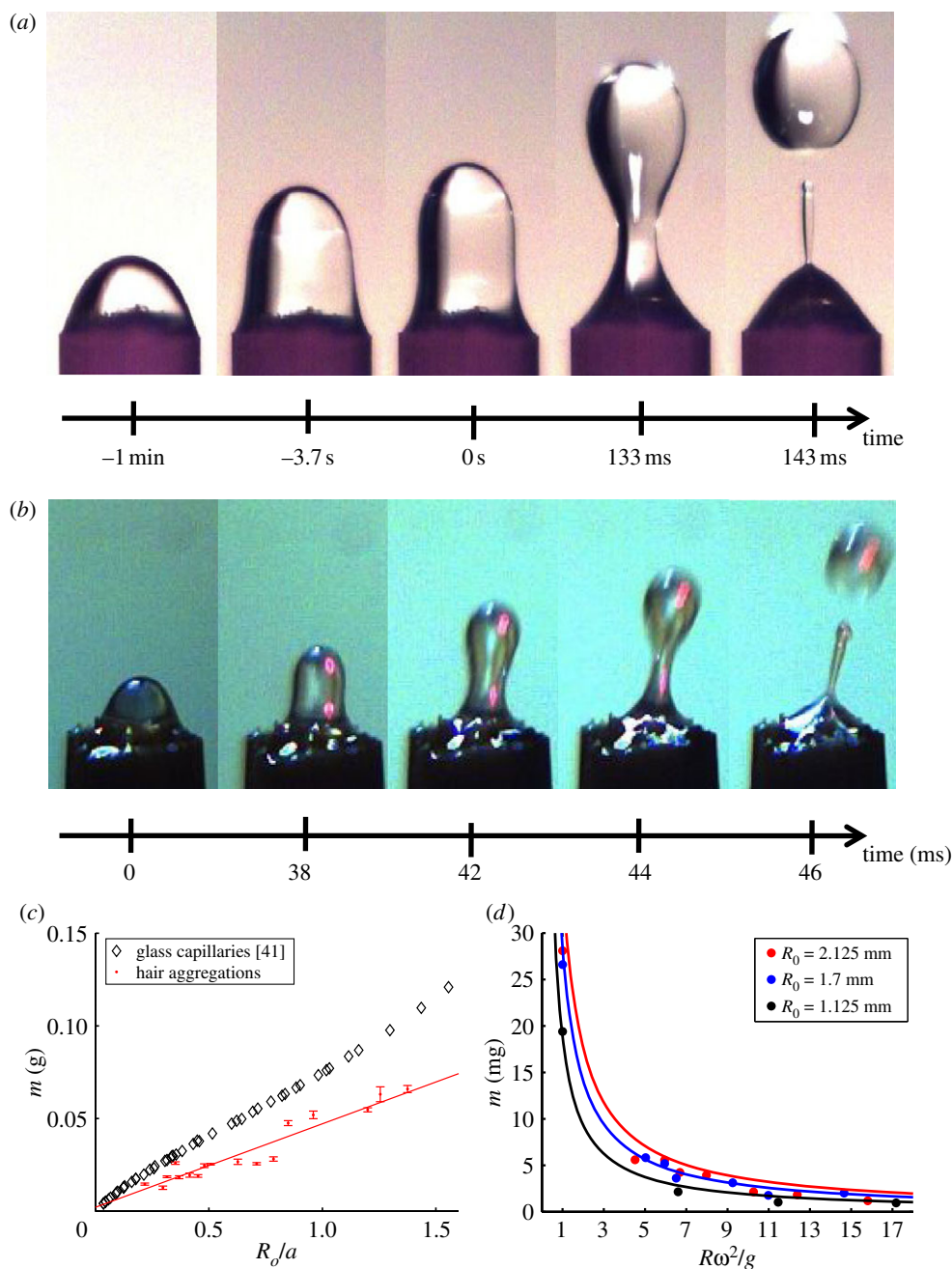


Figure 4. Drop departure from fibre aggregations. (a,b) Video sequences of drop ejection under gravity and due to spinning, respectively. In the latter, centrifugal forces are $R\omega^2/g = 11$ and smaller drops are ejected. (c) The dependence of drop mass m and hair aggregation size R_0 for dripping under gravity. The mass of drops dripping from glass capillaries is shown for comparison. (d) The relation between drop mass and dimensionless centrifugal acceleration for three hair aggregations of varying diameters. Best fits in (c,d) are given by equation (3.3) using $F(R_0/a) = 0.4$. (Online version in colour.)

applications [37,38]. In these cases, drop size can be very carefully controlled. The conditions for drop detachment from a capillary are given by Tate's Law [39,40]: to detach, a drop's effective weight mG must overcome the surface tension force σR_0 binding the drop to adjacent hairs, where m is the drop's mass, $\sigma = 72$ dynes cm^{-1} is the surface tension of water and R_0 is the paintbrush radius. During normal dripping $G = g$, the acceleration of gravity. During shaking, drops have a larger effective weight owing to centrifugal forces, $F_{\text{cent}} = mR\omega^2$, which, for the mammals, we have filmed can be 10–70 times gravity (table 1). As shown in figure 4a,b, the

high centrifugal forces cause extruded drops to be smaller; we will see later that they result in far more fluid extracted than simply by gravity.

Note that because our device spins at a constant speed, our experiments do not account for the dynamics of oscillating, pendulum-like motion, which may also act to eject drops. The relative magnitudes of centrifugal to acceleration forces are comparable, $F_{\text{accel}}/F_{\text{cent}} = |(d\omega/dt)/\omega^2| = A^{-1} \approx 0.65$, suggesting that drops are likely to be shed by a combination of both mechanisms; nevertheless, we consider only centrifugal forces in our analysis.

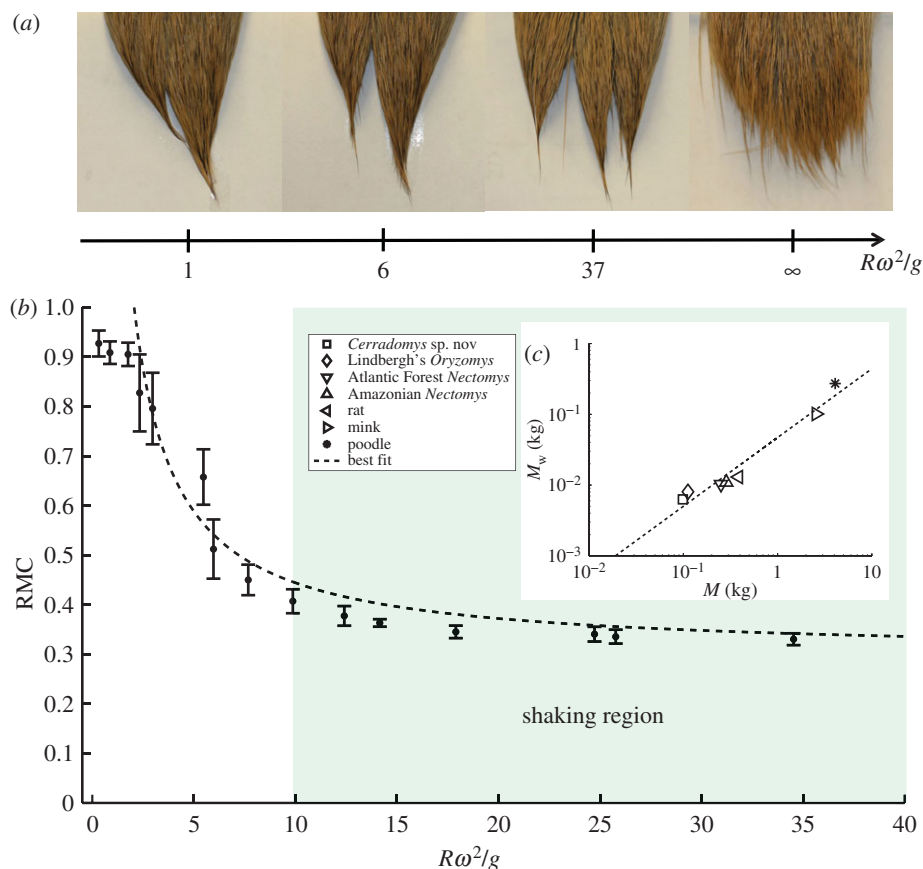


Figure 5. Properties of hair clumps measured using our wet-dog simulator. (a) The separation of wet aggregations upon spinning. (b) The relation between RMC and non-dimensional centrifugal acceleration. Error bars indicate the standard deviation of measurement. (c) Mass of water held on a wet animal's body versus animal mass. Data for wet and dry masses for *Cerradomys* sp. nov, Lindbergh's *Oryzomys*, Atlantic forest *Nectomys* and Amazonian *Nectomys* were collected by Santori *et al.* [13], while the mink was gathered from Korhonen & Niemela [14]. (Online version in colour.)

3.5. Tate's Law applied to hair clumps

Our experiments reveal that drops formed by wet paintbrushes very consistently satisfy Tate's Law. Figure 4c shows the dependency of drop mass on clump size R_0 under gravity: drop mass is linearly proportional to clump size, as shown by the red points. Note this behaviour is similar to that shown previously for capillary tubes, as shown by the diamonds in figure 4c. Figure 4d shows the dependency of drop mass on rotational speed for three clump sizes ($R_0 = 1.1, 1.7, 2.1$ mm): drop mass is inversely proportional to centrifugal acceleration $R\omega^2$. Together, these findings demonstrate the modified Tate's Law for the mass of drops released,

$$m = \left(\frac{2\pi\sigma R_0}{R\omega^2} \right) F\left(\frac{R_0}{a}\right), \quad (3.3)$$

where σ is surface tension of water, ρ is density and $a = \sqrt{\sigma/\rho g} \approx 2.7$ mm is capillary length. For the best fit trend lines in figure 4c,d, we estimate the correction factor [41] for hair clumps as a constant function, $F(R_0/a) = 0.4$. The correction factor for an analogous system, glass pipettes, was previously determined to be a non-constant function by Harkins & Brown [41]. Measurements of this function in our experiments yielded a small range, from 0.3 to 0.6, indicating the low impact

of approximation as a constant function (see electronic supplementary material). As shown by the agreement between the solid lines and the experimental data in figure 4c,d, equation (3.3) well predicts the mass of the drops shed for an animal shaking at a fixed rotational velocity ω with hair clumps of size R_0 .

We surmise that the drying of animals proceeds as follows. Large drops, whose size are on the order of the capillary length, naturally depart the animal under to gravity as in figure 4a. However, thin films of water on the hairs and the smallest drops remain attached and so can be removed only by shaking, as shown in figure 4b. Equation (3.3) shows that if an animal increases its rotational velocity and so its centrifugal force compared with gravity, it may extend the range of drop masses shed. However, at a given rotational velocity, the residual drop masses left behind after shaking, shown in figure 4a,b, may be too small to be ejected by centrifugal forces, and so may remain attached to the animal.

3.6. Prediction of shaking allometry

We may simplify Tate's Law to formulate a 'wet-dog shake rule', an allometric relation between animal mass and shaking frequency. Formulation of such a scaling law requires determining which variables within equation

(3.3) are independent of animal mass and so may be fixed as constant. We consider each of the five variables in turn (σ , A , m , R_0 , f), turning first to variables that are independent of animal mass, as found either in our experiments or in literature. Clearly, material properties of the fluid such as surface tension σ are independent of animal mass. In our experiments, we observe shaking amplitude A varies over a range of 60–110° without clear trends in animal mass. We find hair properties such as hair length and density do not vary systematically across mammal mass (see electronic supplementary material). Thus, we fix wet hair clump radius, which depends primarily on hair length and density.

The remaining variables in equation (3.3) are the radius R , which is an independent variable, and two dependent variables, the chosen shaking frequency f and the shed drop size m . The shed drop mass is a function of both the radius and the frequency of shake. In particular, over the range of $R\omega^2/g = 10$ –70 for animals studied (table 1), equation (3.3) predicts drop mass will vary by a factor of 7. This amount is low in comparison with the variation in other variables considered. Variation in animal radius R is a factor of 24 (from 1 to 24 cm); moreover, variation in the square of frequency (4–30 Hz) is a factor of 50. Each of these factors are greater than seven. Moreover, their combined variation of $R\omega^2$ varies by an even larger factor of 1200 if R and ω were to vary independently. Thus, we assume that drop mass is constant and proceed with our scaling to determine the relation between frequency and radius.

We apply an allometric relation relating animal mass and radius previously found by McMahon & Bonner [42]: animals are nearly isometric according to Kleiber's Law such that $M \sim R^{8/3}$. Applying this law, the resulting scaling relation between animal mass and shaking frequency is

$$f \sim M^{-3/16}. \quad (3.4)$$

By shaking at such frequencies, furry animals act like a high-pass filter, causing drops above a critical size m to eject. This critical drop size is determined by the scaling pre-factor in equation (3.4), which depends on the drop's surface tension and density according to equation (3.3). It is noteworthy that our predicted exponent of -0.19 ($R^2 = 0.92$) is close to the observed value of -0.22 . Our exponent is within the 99.8 per cent confidence intervals for our experimental best fit, indicating that there is only a 0.2 per cent chance that our the predicted exponent is different from the measured one. We attribute this small discrepancy, which scales as an infinitesimal $M^{0.03}$, to simplifications in our model, most likely regarding animal radius.

The increase in shaking speed for smaller animals is important in compensating for their smaller radius. This tuning of shaking frequency with body size is necessary to generate the large centrifugal forces required to shed drops, $R\omega^2/g = 10$ –70 gravities, for the animals listed in table 1. If, for example, all animals shook at the frequency of a dog, the smallest animals would have insufficient force to remove drops: for example, a mouse shaking at 4 rather than 30 Hz would generate only 1 gravity of centrifugal acceleration, and would remain just as wet.

3.7. *Shaking animals achieve similar residual moisture content*

In our experiments with paintbrushes, we found that the frequencies required for drop detachment depend on clump size R_0 . We now use experiments with real animal fur to measure how clump size changes during longer durations (30 s) of shaking. Figure 5*a* shows the hair clump configurations at various speeds of rotation for a 6.3 cm² square sample of deer fur. As rotation speed increases so that centrifugal forces increase from 1 to 40*g*, the clumps separate into a cascade of smaller clumps. By weighing these clumps, we find this separation is accompanied by an exponentially increasing difficulty in drying, which gives further rationale for the frequencies used by the animals.

Figure 5*b* shows the relation between the centrifugal forces applied and the remaining moisture content RMC within our deer fur sample. We define RMC as the ratio of the post-shake mass to the initial mass of water in the clump, following by textile-drying engineers [43]. In figure 5*b*, the limiting RMC values of $D = 30$ per cent show excellent agreement with our measurements of $\text{RMC} = 0.31 \pm 0.12$ ($N = 10$) on live rats, suggesting our experiments with spun deer hair are representative of shaking live animals. From the combination of these results, we conclude that 30 per cent RMC is the lowest level of dryness obtainable using shaking. Moreover, the lowest RMC values of 0.3–0.4 values occur for speeds in which the associated centrifugal force is

$$\frac{R\omega^2}{g} > 10, \quad (3.5)$$

as indicated in the shaded region in figure 5.

As shown in table 1, all shaking mammals in our study have centrifugal forces in the range of 10–70, a relatively small range considering the four orders of magnitudes of mass of the animals. Notably, this range of forces coincides with the region of peak dryness given by equation (3.5), which was found independently with our wet-dog simulator. We conclude that animals shake to achieve nearly equal and maximal levels of dryness.

3.8. *Physical basis of residual moisture content*

We may rationalize the trends observed in figure 5*b*, beginning with the initial RMC of deer fur under gravity. The mass of water in the hair is proportional to the corresponding water column height within the fur. When fur is initially wetted, surface tension competes with elasticity to bring the water column between the hairs to an equilibrium height [26] of $H_{\text{initial}} = L - (\frac{9}{2}d^2 L_{\text{EC}}^2 / \cos \theta_e)^{1/4}$, where hair length in the deer fur sample $L \approx 40$ mm, hair follicle radius $b \approx 200$ μm , inter-hair spacing $d \approx 0.028$ cm, elastocapillary length is $L_{\text{EC}} = \sqrt{EI/\sigma b} = 57$ cm, the Young's modulus is $E = 3.7$ GPa, $I = \pi b^4/4 \approx 1.26 \times 10^{-3}$ mm⁴ is the area moment of inertia and $\theta_e = 60^\circ$ is the equilibrium contact angle of water on hair [34]. We find this model is fairly accurate for our 6.3 cm² square sample of deer fur. Given its combined water column cross-sectional area A_{fur} of 2.4 cm² (measured

by the area of space between the furs), we predict the hairs will retain $m_{\text{initial}} = \rho H_{\text{initial}} A_{\text{fur}} = 4.4$ g of water, whereas it held 4.7 g in our experiments. Thus, elastocapillarity theory is sufficient to account for the wet weight of deer fur under gravity, and the discrepancy between experiment and theory suggests water may soak into the hair fibres.

When fur is spinning, the associated centrifugal force competes with surface tension to decrease the height of the water column to a modified Jurin's height $H = 2\sigma \cos \theta_e / \rho R \omega^2 d$. Using the definition of RMC, we may write $\text{RMC} = H/H_{\text{initial}} + D$, where D is a free parameter used for fitting the asymptote in figure 5*b*. This parameter D cannot be predicted with our simple model, as it represents the moisture that soaks into the rough surfaces of the hair and skin, and cannot be removed even under extreme centrifugal forces [44–47]. The remaining moisture content simplifies to

$$\text{RMC} = \frac{C}{R\omega^2} + D, \quad (3.6)$$

where $C = 2\sigma \cos \theta_e / \rho d H_{\text{initial}} = 14.2 \text{ m s}^{-2}$ and $D = 0.3$. Our measurements of RMC of deer fur in figure 5*b* show a power law qualitatively consistent with equation (3.6), having a goodness of fit $R^2 = 0.93$ within the range of $R\omega^2/g = 2$ –35. For small rotation speeds $R\omega^2/g < 2$, RMC is sigmoidal and outside the scope of our model, owing to elastic and gravitational forces becoming comparable with centrifugal forces in this regime.

Using our measured trends in moisture content in figure 5*b*, we may quantify the benefits of the animal's loose dermal tissue, observed in figure 1*c*. Previously, we found loose dermal tissue increases the shake amplitude by threefold, and thus the speed of shaking by ninefold. If dermal tissue were tight rather than loose (as on humans), animal shaking frequencies would cause RMC values to remain close to 1, indicating the animal would remain wet. Thus, an important role of the loose dermal tissue is to increase the efficacy of the shake, as shown by the sensitivity of the RMC to changes in skin speed.

3.9. Shaking energy expenditures

We may assess the effectiveness of shaking by comparing the energetic costs of shaking versus evaporating the water. The shaking energy can be estimated as the peak kinetic energy for simple harmonic motion, given by $E_{\text{shake}} = \frac{1}{2} M (R\omega)^2$. If animals can shake 70 per cent of their water off, as shown in §3.7, the energy required to evaporate that mass of water is given by $E_{\text{evap}} = 0.42 \lambda M_w$, where M_w is the mass of the water on the animal and λ is the heat of vaporization of water. The coefficient 0.42 is a product of 0.6, the fraction of energy needed from the animal to evaporate water [16] and 0.7, the fraction of water an animal can shake off as found in our experiments.

Figure 5*c* shows the relation between an animal's body mass M and the mass of water in its fur, M_w . Data for seven mammals were found by combining our own measurements of wet animals along with others [13,14]. The trend follows the power law $M_w = 0.047 M^{0.97}$, where M and M_w are both in kilograms, with high

accuracy ($R^2 = 0.95$, $N = 7$). The mass of the water held in the fur is approximately 3–10% of the animal's body mass for the masses considered (0.1–4 kg).

We combine the above energetic estimates with our measurements of animal frequency to calculate an efficacy of shaking. We define this efficacy as the ratio of the energy expended to shake to the energy expended to air-dry as $\eta = E_{\text{shake}}/E_{\text{evap}}$. We find that over the four orders of magnitude of mass for animals studied, this efficacy has a small range from 10^{-4} to 10^{-3} . In this range, all values are far less than one, indicating the great energy savings achieved by shaking.

4. DISCUSSION

4.1. Predictions based on power

In tests with animal hair, we found the observed frequencies were capable of drying the animal appreciably, as defined by removing 70 per cent of its accumulated water. Furthermore, we found that increased speeds imparted to the fur would achieve diminishing return. Thus, the animal obtains a reasonable amount of dryness without expending an excess of energy. The work per shake W of an animal [42] scales as the mass of its muscles ($W \sim M$). The kinetic energy expended per shake is $W \sim MR^2 \omega^2 \sim MR^2 f^2$; thus if animals shook as fast as possible, their frequency would scale as, $f \sim R^{-1} \sim M^{-3/8}$. We note that our observed scaling exponent of -0.22 falls between the minimum frequencies for drop release (-0.19) and the maximum frequencies based on power output (-0.375). Thus, it may not be possible for animals to dry further because they may be at the upper limits of shaking speed they can generate. In studies of galloping, stride frequencies of small mammals varied from 2 to 9 strides per second, whereas the frequencies of shaking are faster (4–30 shakes per second). Studies regarding drug-induced tremors in mice reported shivering frequencies to be very close to shaking frequencies at 25 shakes per second [48], which is quite possibly at the limits of oscillatory motion of muscle.

4.2. Comparison with other scaling laws

Our measurements of shaking frequency may be related to other frequencies associated with animal movement. Stahl measured the heartbeat frequency [49] of resting animals scaling as $f_{\text{hb}} \sim M^{-0.25}$. Joos *et al.* [50] found that the wing beat frequency in bees scales with the bee's mass as $f_{\text{wb}} \sim M^{-0.35}$. Heglund [51] found frequency, in the trot–gallop transition, for mice, rats, dogs and horses, scales as $f_{\text{trot}} \sim M^{-0.14}$. He noticed, for all animals tested, stride frequency became asymptotic, changing less than 10 per cent as the animals increased their speed from the trot–gallop transition to their maximum. These power law scalings are comparable in exponent to the ones we measured for shaking animals, possibly because similar muscles are used to power both locomotion and shaking.

4.3. Scaling frequency with body radius

In predicting a scaling for frequency, care must be taken in choosing an appropriate independent variable. There

are two choices to characterize body size, radius and mass. When choosing body mass, our model fits the experimental results quite well. Rewriting our model, equation (3.4), in terms of frequency and body radius, yields $f \sim R^{-1/2}$. This result is in high variance with respect to experimental data in table 1, which yields $f \sim R^{-0.77}$ ($R^2 = 0.96$). This discrepancy arises from approximating body proportion with a single circumference measurement around the shoulders. However, this is not the only region in need of drying. In fact, other regions of the animal will have a different characteristic radius. Consequently, an animal's mass, which scales as its volume, more accurately captures the average radius of the animal that the drops encounter during shaking. This reasoning explains why our scaling with respect to animal mass ultimately yielded a closer fit to experimental data.

4.4. Predictions and exceptions

We hypothesize shaking when wet is an ancient survival mechanism, dating back to the emergence of furry mammals. Many Pleistocene mammals were covered with hair. Giant beavers [52], similar in size to a black bear, and short-faced bears [53], similar in size to grizzlies, would have probably shaken similarly to their modern counterparts. Although the ability to shake probably spans generations of furry mammals, it is not a characteristic of all mammals, even of those today. The largest mammals' thermal mass is a likely cause for its inability to shake. In addition, aquatic mammals and those covered with a hard shell, such as an armadillo, have no need to shake dry. Other animals with specialized slow lifestyles such as the giant sloths may not possess the speed to initiate a shake.

Hairless mammals may have no shaking instinct. While filming, we observed hairless guinea pigs did not shake, but only shivered. In personal observations, some species such as the sparsely haired warthog spend their days bathing in muddy water. We expect that nearly hairless species, adapted to hot environments, have not developed the behaviour to shake when wet.

We saw earlier that loose dermal tissue played a role in increasing the speed, force and efficacy of the shake. This constraint may also prevent certain species from shaking. For instance, while humans do not generally have loose dermal tissue, some humans can use their long hair to shed water. This technique involves repeated motion of the head and upper torso in the dorsoventral plane to whip water from their hair. Although the head is oscillated at the low frequencies of only 1–2 Hz, the hair length aids to increase the amplitude and speed at which hair tips are whipped, and consequently the ensuing dryness.

5. CONCLUSION

In this study, we demonstrated that reciprocal high-speed twisting commonly observed in dogs has a broad generality among mammals. We found that drops remain adhered to a wet animal's hair due to the forces of surface tension. To eject drops and achieve dryness levels of 30 per cent, we found animals generated centrifugal forces equivalent to 10–70. In order

for animals of variable size to attain this magnitude of force, we predicted animals must shake at frequencies of $f \sim M^{-3/16}$, which was similar to experimentally measured frequencies. We conclude animal frequency is tuned to (i) the animal's size and (ii) the properties of water, namely surface tension and density, which set the magnitudes of the centrifugal and capillary forces in our model. Consequently, such mechanisms work poorly when animals are subjected to fluids with properties different from water such as crude oil, whose wetting properties and inability to evaporate prevents the shake from being effective.

Animals were provided by Zoo Atlanta, the local park, and neighbouring laboratories at our institution, and filmed according to IACUC protocols A09036 and A10066.

The authors thank R. DeBernard, P. Foster, L. O'Farrell for laboratory assistance, J. Aristoff for useful discussions, and the NSF (PHY-0848894) for support.

REFERENCES

- 1 Neinhuis, C. & Barthlott, W. 1997 Characterization and distribution of water-repellent, self-cleaning plant surfaces. *Ann. Bot.* **79**, 667–677. (doi:10.1006/anbo.1997.0400)
- 2 Bush, J. W. M., Hu, D. L. & Prakash, M. 2008 The integument of water-walking arthropods: form and function. *Adv. Insect Physiol.* **34**, 117–192. (doi:10.1016/S0065-2806(07)34003-4)
- 3 Timacheff, S. 2008 *Canon EOS digital photography photo workshop*. Indianapolis, IN: Wiley Publishing Inc.
- 4 Ferri, F., Smith, P., Lemmon, M. & Rennó, N. 2003 Dust devils as observed by Mars Pathfinder. *J. Geophys. Res.* **108**, 1–7. (doi:10.1029/2000JE001421)
- 5 Van Rooijen, J. 2005 Dust bathing and other comfort behaviours of domestic hens. In *Welfare of laying hens in Europe—reports, analyses and conclusions* (eds G. Martin, H. H. Sambras & A. Steiger), pp. 110–123. Munich, Germany: Internationale Gesellschaft für Nutztierhaltung.
- 6 Sokolov, V. 1982 *Mammal skin*. Berkeley, CA: University of California Press.
- 7 Romanenko, E. & Sokolov, V. 1987 Wettability of the coat of the northern fur seal. *Doklady Akademii Nauk SSSR* **297**, 990–994.
- 8 Fish, F., Smelstoy, J., Baudinette, R. & Reynolds, P. 2002 Fur does not fly, it floats: buoyancy of pelage in semi-aquatic mammals. *Aquat. Mamm.* **28**, 103–112.
- 9 Weisel, J., Nagaswami, C. & Peterson, R. 2005 River otter hair structure facilitates interlocking to impede penetration of water and allow trapping of air. *Can. J. Zool.* **83**, 649–655. (doi:10.1139/z05-047)
- 10 Spruijt, B., Van Hooff, J. & Gispen, W. 1992 Ethology and neurobiology of grooming behavior. *Physiol. Rev.* **72**, 825–852.
- 11 Ortega-Jimenez, V. & Dudley, R. 2011 Aerial shaking performance of wet Anna's hummingbirds. *J. R. Soc. Interface* **70**, 1093–1099. (doi:10.1098/rsif.2011.0608)
- 12 Haldane, J. 1956 On being the right size. *World Math.* **2**, 952–957.
- 13 Santori, R., Vieira, M., Rocha-Barbosa, O., Magnan-Neto, J. & Gobbi, N. 2008 Water absorption of the fur and swimming behavior of semiaquatic and terrestrial oryzomine rodents. *J. Mamm.* **89**, 1152–1161. (doi:10.1644/07-MAMM-A-327.1)

- 14 Korhonen, H. & Niemela, P. 2002 Water absorption and the drying and cooling rates in mink (*Mustela vison*) following simulated diving. *Anim. Sci.* **74**, 277–284.
- 15 Webb, D. & King, J. 1984 Effects of wetting of insulation of bird and mammal coats. *J. Therm. Biol.* **9**, 189–191. (doi:10.1016/0306-4565(84)90020-2)
- 16 Bakken, G. 1976 A heat transfer analysis of animals: unifying concepts and the application of metabolism chamber data to field ecology. *J. Theor. Biol.* **60**, 337–384. (doi:10.1016/0022-5193(76)90063-1)
- 17 Schmidt-Nielsen, K. 1997 *Animal physiology: adaptation and environment*. Cambridge, UK: Cambridge University Press.
- 18 Erasmus, H. 2008 Determination of some blood parameters in the African lion (*Panthera leo*). PhD thesis. University of the Free State.
- 19 Sterndale, R. 1884 *Natural history of the mammalia of India and Ceylon*. Bombay, India: Thacker, Spink & Co.
- 20 Rogers, L. 1976 Effects of mast and berry crop failures on survival, growth, and reproductive success of black bears. *Transactions, Forty-first North American Wildlife and Natural Resources Conference, 21–25 March 1976, Washington DC*, vol. 41, pp. 431–438. Washington DC: Wildlife Management Institute.
- 21 Swenson, J., Sandegren, F. & SO-Derberg, A. 1998 Geographic expansion of an increasing brown bear population: evidence for presaturation dispersal. *J. Anim. Ecol.* **67**, 819–826. (doi:10.1046/j.1365-2656.1998.00248.x)
- 22 Costello, C. *et al.* 2003 Relationship of variable mast production to american black bear reproductive parameters in New Mexico. *Ursus* **14**, 1–16.
- 23 Blanchard, B. 1987 Size and growth patterns of the Yellowstone grizzly bear. *Bears Biol. Manage.* **7**, 99–107. (doi:10.2307/3872615)
- 24 Nagy, J., Kingsley, M., Russell, R. & Pearson, A. 1984 Relationship of weight to chest girth in the grizzly bear. *J. Wildl. Manage.* **48**, 1439–1440. (doi:10.2307/3801815)
- 25 Koprowski, J. 1991 Response of fox squirrels and gray squirrels to a late spring-early summer food shortage. *J. Mammalogy* **72**, 367–372. (doi:10.2307/1382108)
- 26 Bico, J., Roman, B., Moulin, L. & Boudaoud, A. 2004 Adhesion: elastocapillary coalescence in wet hair. *Nature* **432**, 690. (doi:10.1038/432690a)
- 27 Kim, H. & Mahadevan, L. 2006 Capillary rise between elastic sheets. *J. Fluid Mech.* **548**, 141–150. (doi:10.1017/S0022112005007718)
- 28 Py, C., Bastien, R., Bico, J., Roman, B. & Boudaoud, A. 2007 3D aggregation of wet fibers. *Europhys. Lett.* **77**, 44005. (doi:10.1209/0295-5075/77/44005)
- 29 Gilet, T., Terwagne, D. & Vandewalle, N. 2010 Droplets sliding on fibres. *Eur. Phys. J.* **31**, 253–262. (doi:10.1140/epje/i2010-10563-9)
- 30 Zhao, Y. & Fan, J. 2006 Clusters of bundled nanorods in nanocarpet effect. *Appl. Phys. Lett.* **88**, 103 123–103 123. (doi:10.1063/1.2183735)
- 31 Teerink, B. 2004 *Hair of west European mammals: atlas and identification key*. Cambridge, UK: Cambridge University Press.
- 32 Kamath, Y., Dansizer, C. & Weigmann, H. 1978 Wetting behavior of human hair fibres. *J. Appl. Polym. Sci.* **22**, 2295–2306. (doi:10.1002/app.1978.070220821)
- 33 Lodge, R. & Bhushan, B. 2006 Wetting properties of human hair by means of dynamic contact angle measurement. *J. Appl. Polym. Sci.* **102**, 5255–5265. (doi:10.1002/app.24774)
- 34 Carroll, B. 1989 Droplet formation and contact angles of liquids on mammalian hair fibres. *J. Chem. Soc. Faraday Trans.* **85**, 3853–3860. (doi:10.1039/f19898503853)
- 35 Clanet, C. & Lasheras, J. 1999 Transition from dripping to jetting. *J. Fluid Mech.* **383**, 307–326. (doi:10.1017/S0022112098004066)
- 36 Middleman, S. 1995 *Modeling axisymmetric flows: dynamics of films, jets, and drops*. San Diego, CA: Academic Press.
- 37 Walton, W. & Prewett, W. 1949 The production of sprays and mists of uniform drop size by means of spinning disc type sprayers. *Proc. Phys. Soc. B* **62**, 341. (doi:10.1088/0370-1301/62/6/301)
- 38 Dombrowski, N. & Lloyd, T. 1974 Atomisation of liquids by spinning cups. *Chem. Eng. J.* **8**, 63–81. (doi:10.1016/0300-9467(74)80019-5)
- 39 Tate, T. 1864 On the magnitude of a drop of liquid formed under different circumstances. *Philos. Mag. Ser. 4* **27**, 176–180.
- 40 Rayleigh, L. 1915 The principle of similitude. *Nature* **95**, 66–68. (doi:10.1038/095202d0)
- 41 Harkins, W. & Brown, F. 1919 The determination of surface tension (free surface energy), and the weight of falling drops: the surface tension of water and benzene by the capillary height method. *J. Am. Chem. Soc.* **41**, 499–524. (doi:10.1021/ja01461a003)
- 42 McMahan, T. & Bonner, J. 1983 *On size and life*, p. 158. New York, NY: Scientific American Library.
- 43 Tomlinson, J. & Rizy, T. 1998 Measured impacts of high efficiency domestic clothes washers in a community. Technical report 98781. Oak Ridge, TN: National Laboratory, Energy Division.
- 44 Preston, J., Nimakar, M. & Gundavda, S. 1951 Capillary and imbibed water in assemblies of moist fibres. *Textile Res. J.* **42**, T79–T90.
- 45 Denton, M. 1974 The extraction of water from cotton-yarn packages by centrifugal force. I. Spinning in a basket centrifuge. *J. Textile Inst.* **65**, 409–415. (doi:10.1080/00405007408630112)
- 46 Welo, L., Ziifle, H. & McDonald, A. 1952 Swelling capacities of fibers in water. II. Centrifuge studies. *Textile Res. J.* **22**, 261–273. (doi:10.1177/004051755202200404)
- 47 Carter, D., Draper, M., Peterson, R. & Shah, D. 2005 Importance of dynamic surface tension to the residual water content of fabrics. *Langmuir* **21**, 10 106–10 111. (doi:10.1021/la050583w)
- 48 Ahmed, A. & Taylor, N. 1959 The analysis of drug-induced tremor in mice. *Br. J. Pharmacol. Chemother.* **14**, 350–354. (doi:10.1111/j.1476-5381.1959.tb00255.x)
- 49 Stahl, W. 1967 Scaling of respiratory variables in mammals. *J. Appl. Physiol.* **22**, 453–460.
- 50 Joos, B., Young, P. & Casey, T. 1991 Wingstroke frequency of foraging and hovering bumblebees in relation to morphology and temperature. *Physiol. Entomol.* **16**, 191–200. (doi:10.1111/j.1365-3032.1991.tb00556.x)
- 51 Heglund, N. & Taylor, C. 1988 Speed, stride frequency and energy cost per stride: how do they change with body size and gait? *J. Exp. Biol.* **138**, 301–318.
- 52 Reynolds, P. 2002 How big is a giant? the importance of method in estimating body size of extinct mammals. *J. Mammal.* **83**, 321–332. (doi:10.1644/1545-1542(2002)083<0321:HBIAGT>2.0.CO;2)
- 53 Legendre, S. & Roth, C. 1988 Correlation of carnassial tooth size and body weight in recent carnivores (mammalia). *Hist. Biol.* **1**, 85–98. (doi:10.1080/089129 68809386468)